

T cell panel

Phenotypes:

T cells (CD3⁺)

CD4⁺

CD4⁺CD8a⁺

CD8b⁺

DN

In CD4⁺ and CD8b⁺:

Naive CD27⁺CD45RA⁺

CM CD27⁺CD45RA⁻

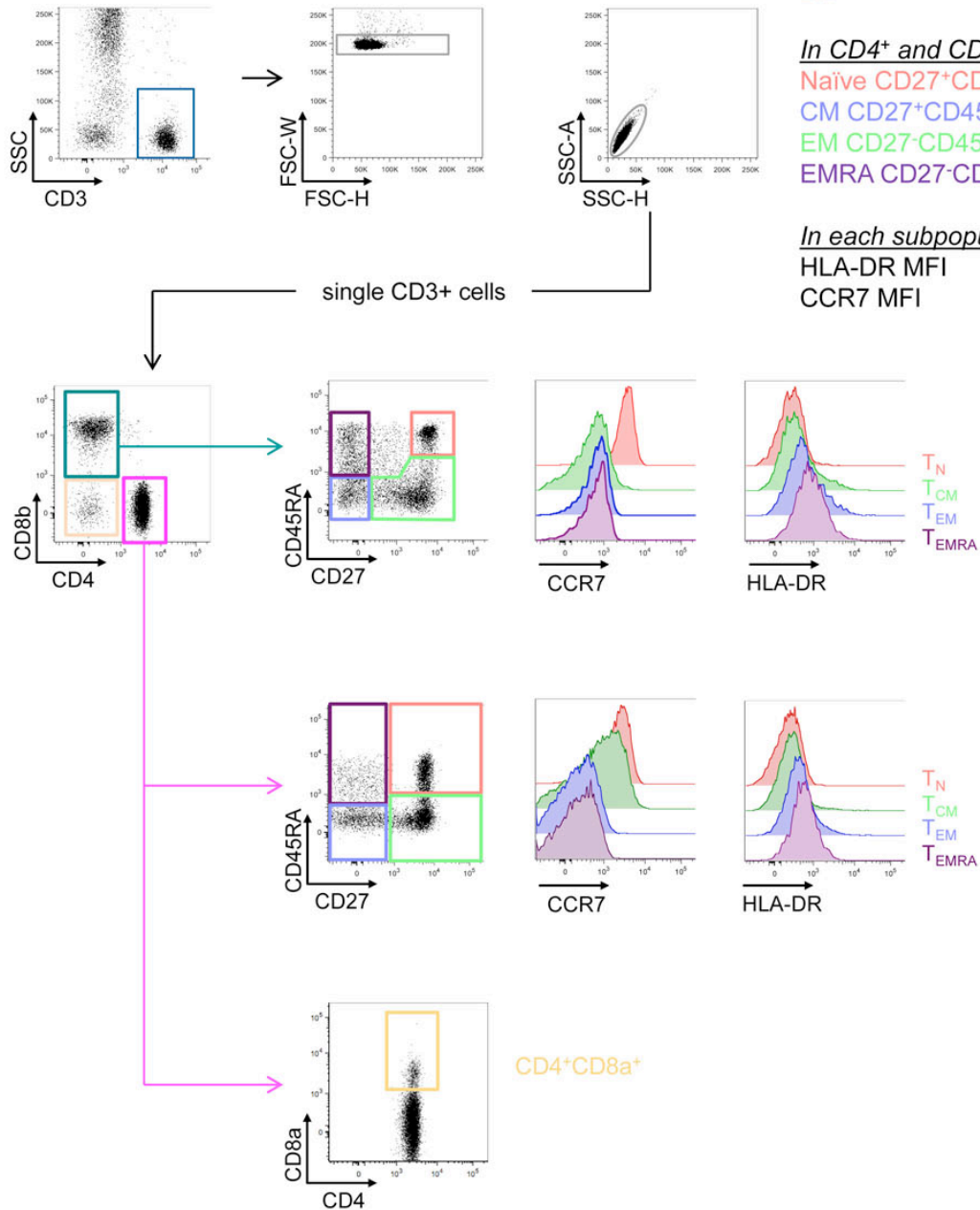
EM CD27⁻CD45RA⁻

EMRA CD27⁻CD45RA⁺

In each subpopulation:

HLA-DR MFI

CCR7 MFI



Supplementary Figure 1

Gating strategy for the T cell flow cytometry panel

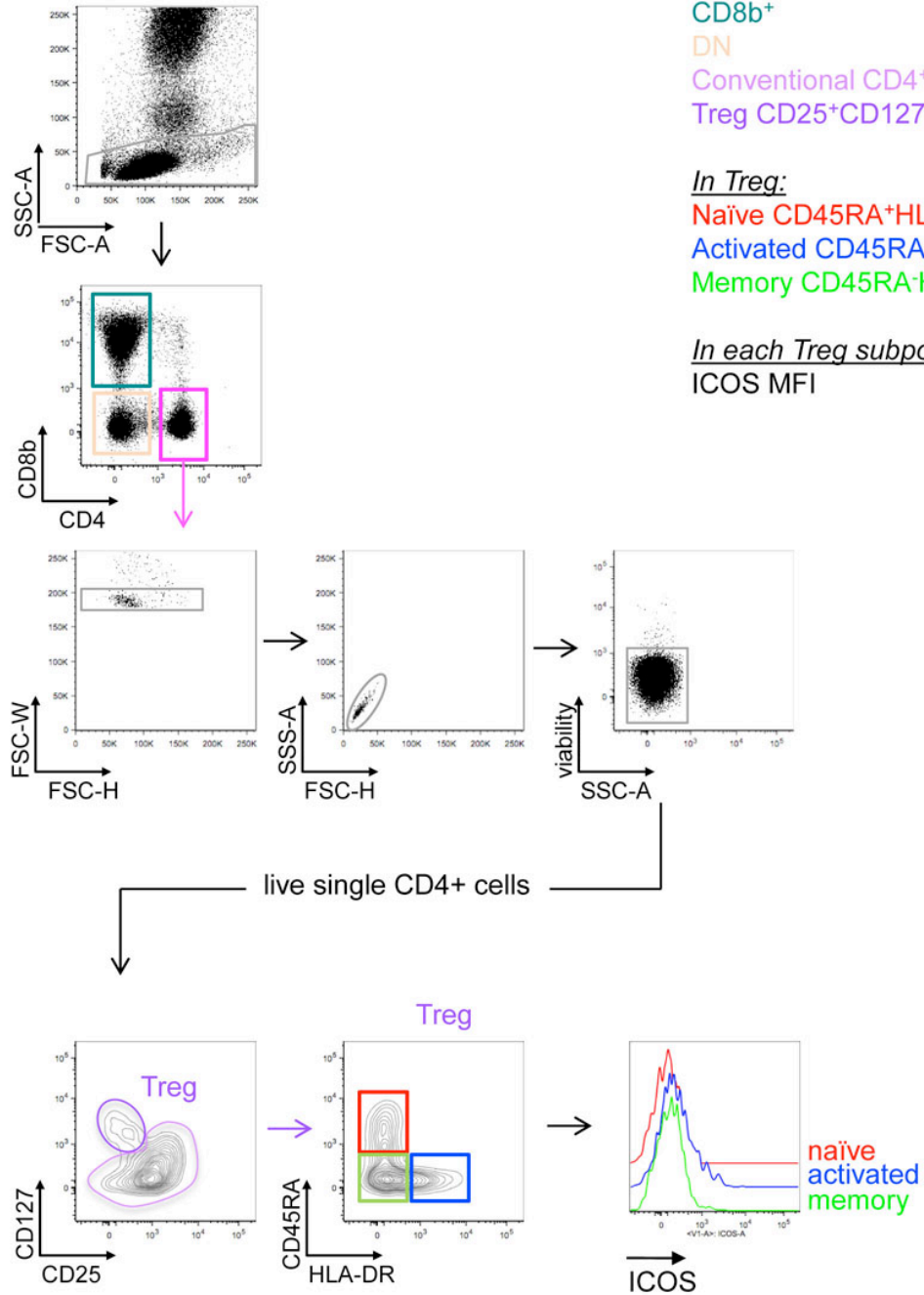
Treg panel

Phenotypes:

CD4⁺
 CD8b⁺
 DN
 Conventional CD4⁺ (CD127⁺)
 Treg CD25⁺CD127⁻

In Treg:
 Naïve CD45RA⁺HLA-DR⁻
 Activated CD45RA⁺HLA-DR⁺
 Memory CD45RA⁻HLA-DR⁺

In each Treg subpopulation:
 ICOS MFI



Supplementary Figure 2

Gating strategy for the T_{reg} cell flow cytometry panel

MAIT/NKT panel

Phenotypes:

T cells (CD3⁺)

TCR $\gamma\delta^+$

CD8b⁺

CD4⁺

DN

In T cell subsets:

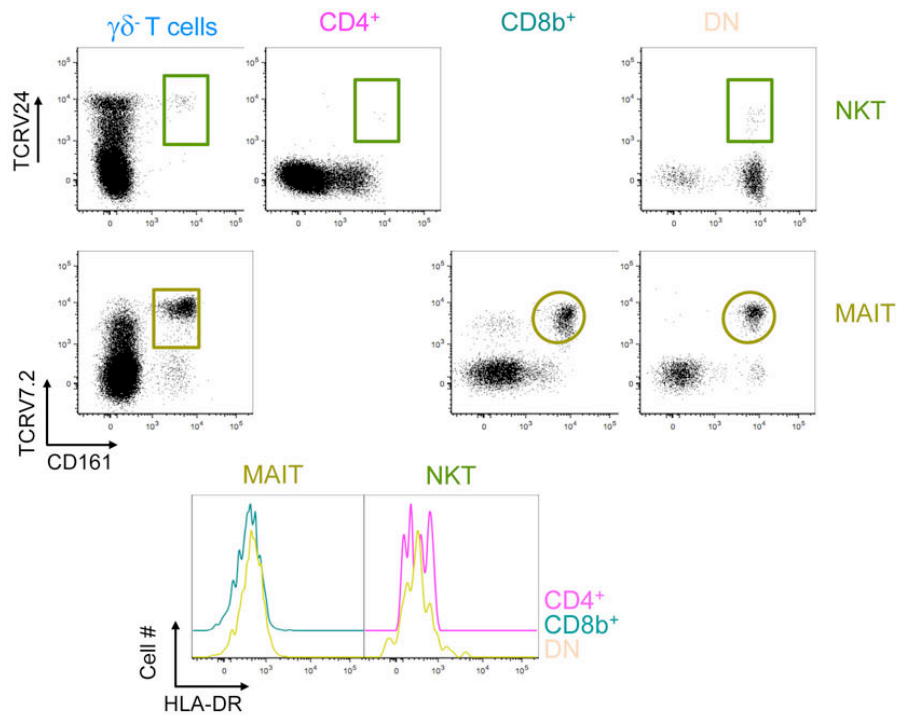
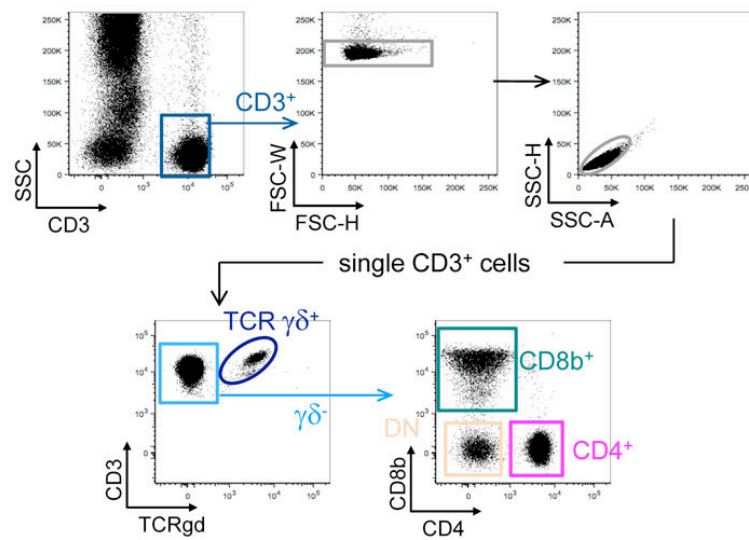
NKT TCRV24⁺CD161^{hi}

MAIT TCRV7.2⁺CD161⁺

In each MAIT & NKT

subpopulation:

HLA-DR MFI



Supplementary Figure 3

Gating strategy for the NKT/MAIT cell flow cytometry panel

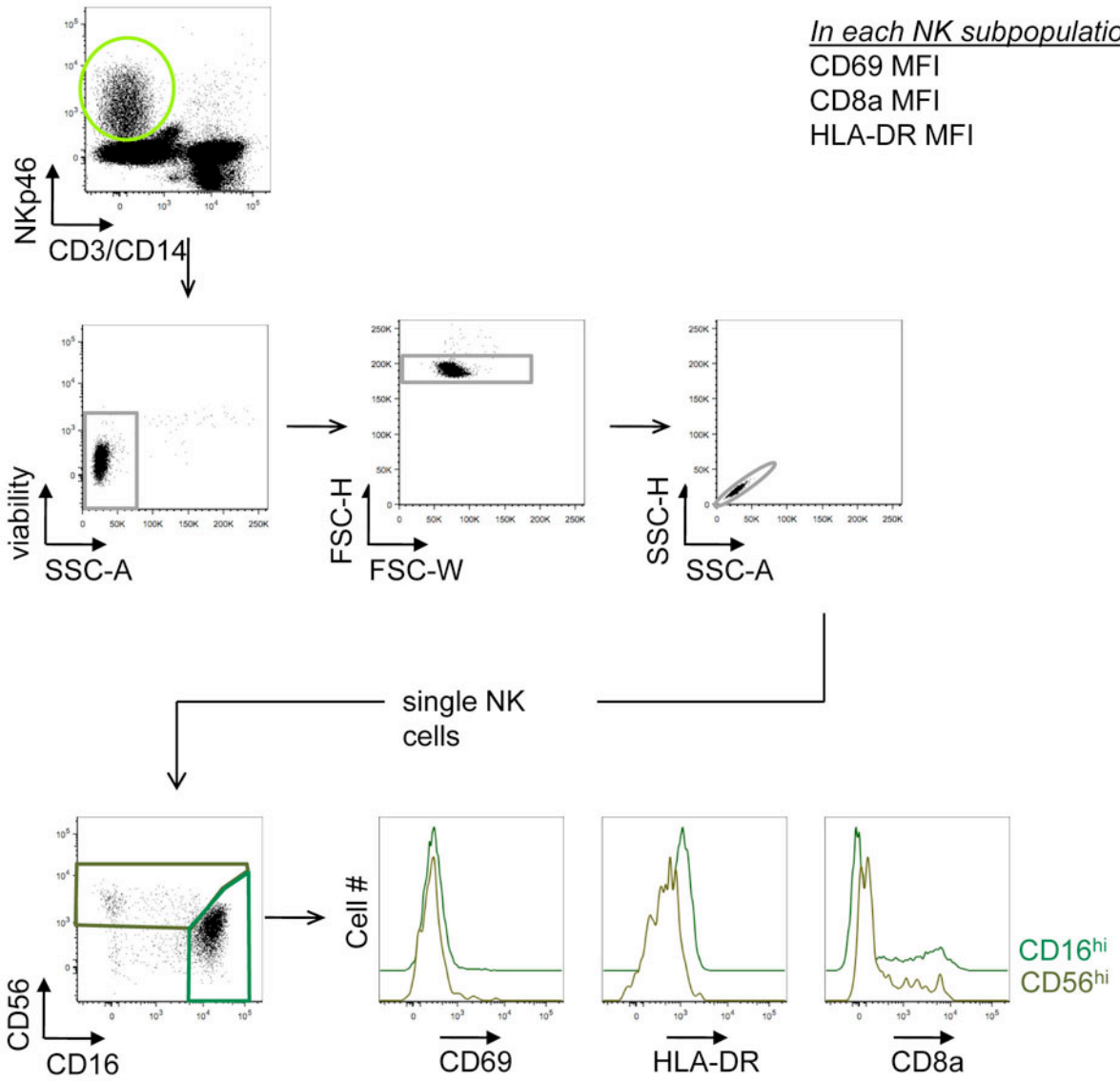
NK panel

Phenotypes:

NK cells (NKp46⁺)
CD56^{hi}CD16^{lo/-}
CD16^{hi}CD56^{lo}

In each NK subpopulation:

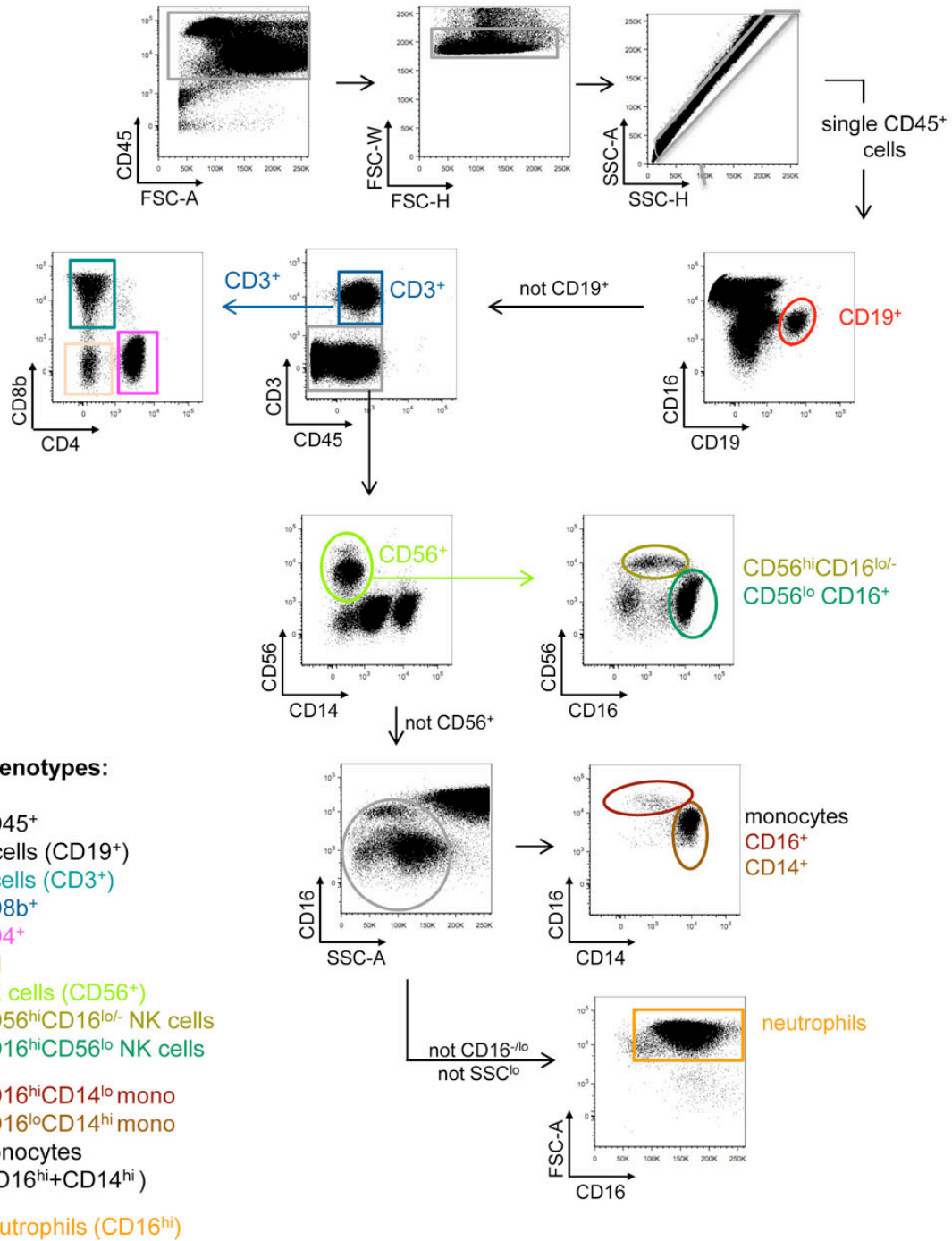
CD69 MFI
CD8a MFI
HLA-DR MFI



Supplementary Figure 4

Gating strategy for the NK cell flow cytometry panel

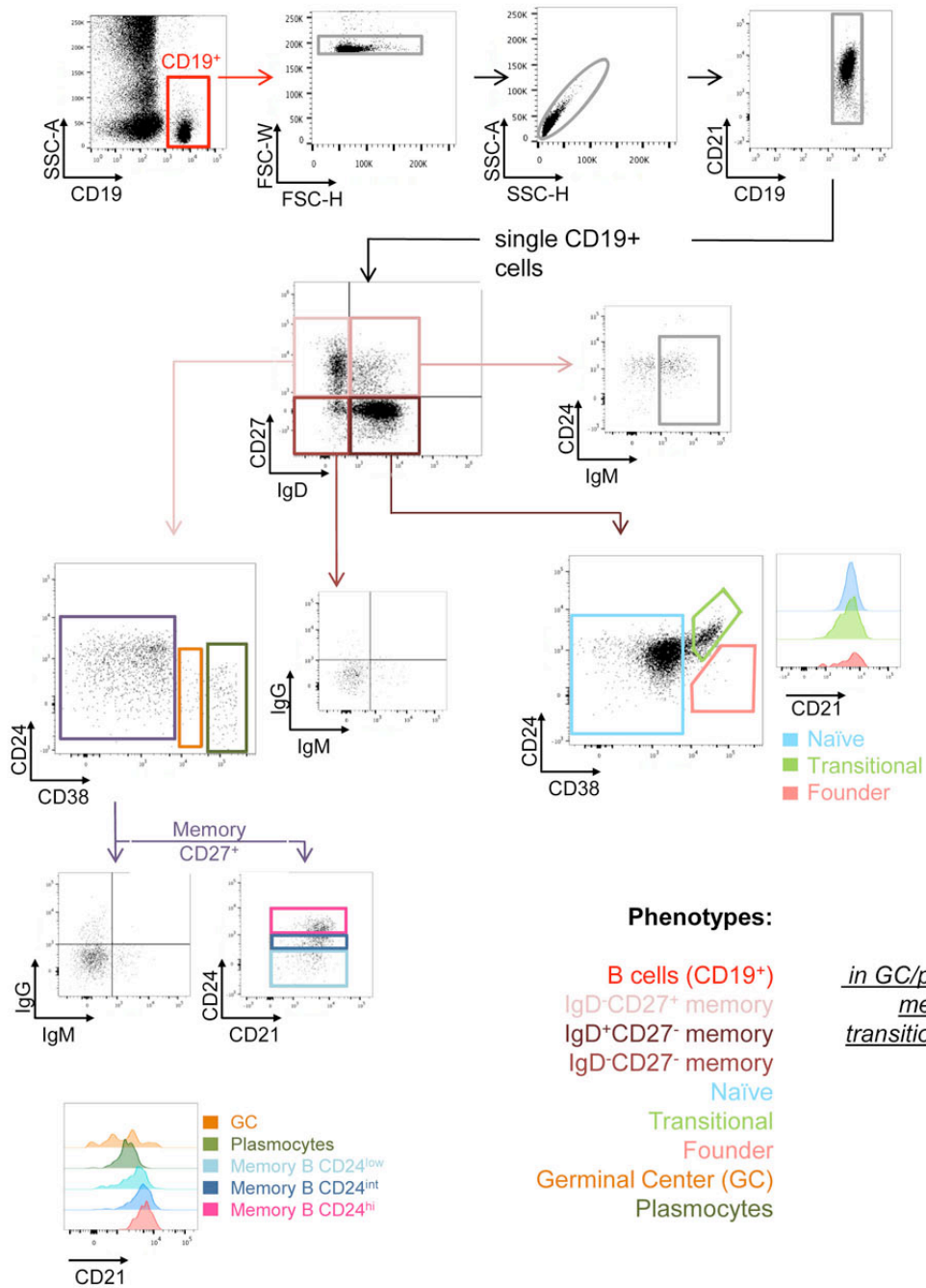
Lineage panel



Supplementary Figure 5

Gating strategy for the lineage cell flow cytometry panel

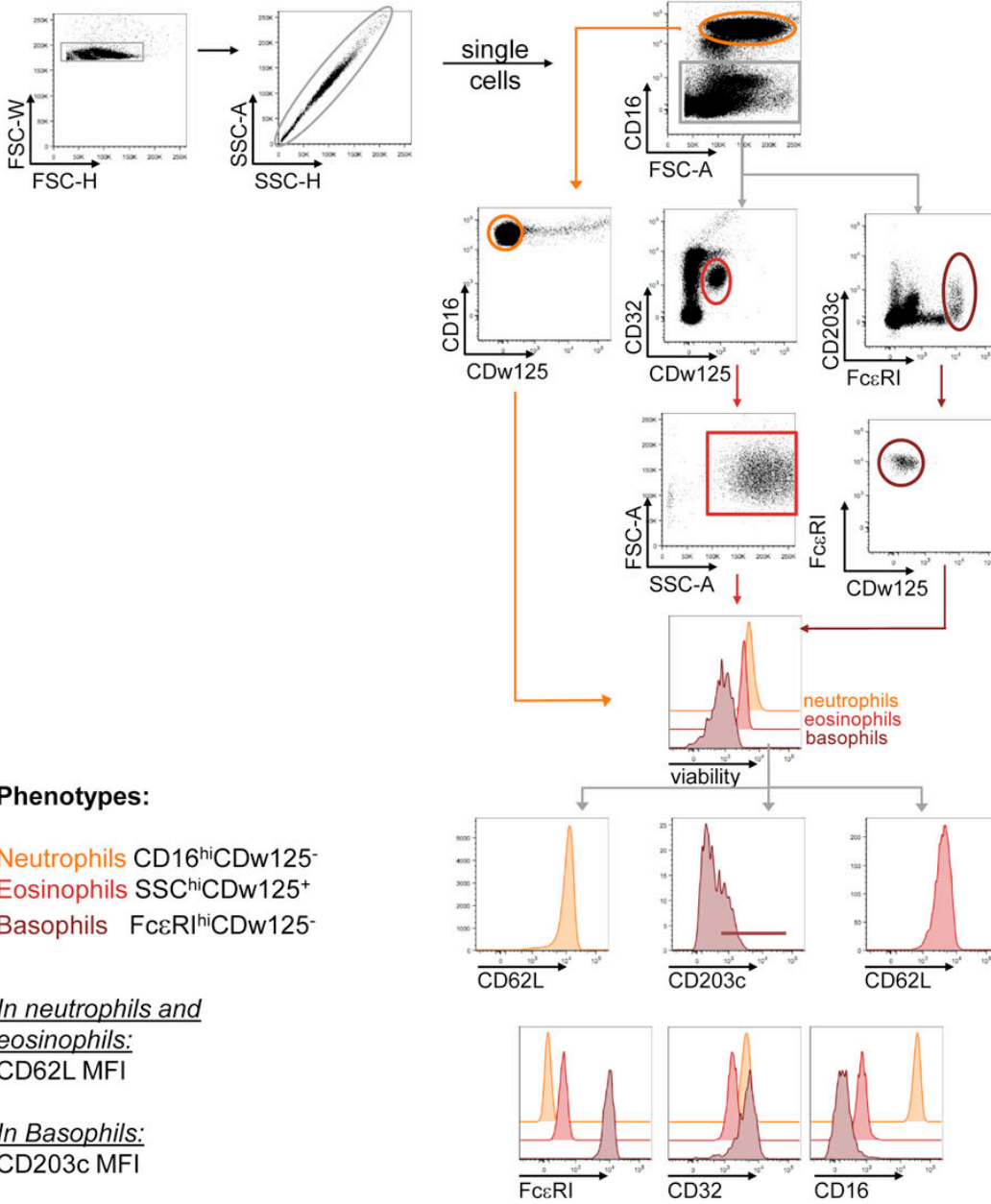
B cell panel



Supplementary Figure 6

Gating strategy for the B cell flow cytometry panel

PMN panel



Phenotypes:

Neutrophils CD16^{hi}CDw125⁻

Eosinophils SSC^{hi}CDw125⁺

Basophils FcεRI^{hi}CDw125⁻

In neutrophils and

eosinophils:

CD62L MFI

In Basophils:

CD203c MFI

In each population:

FcεRI MFI

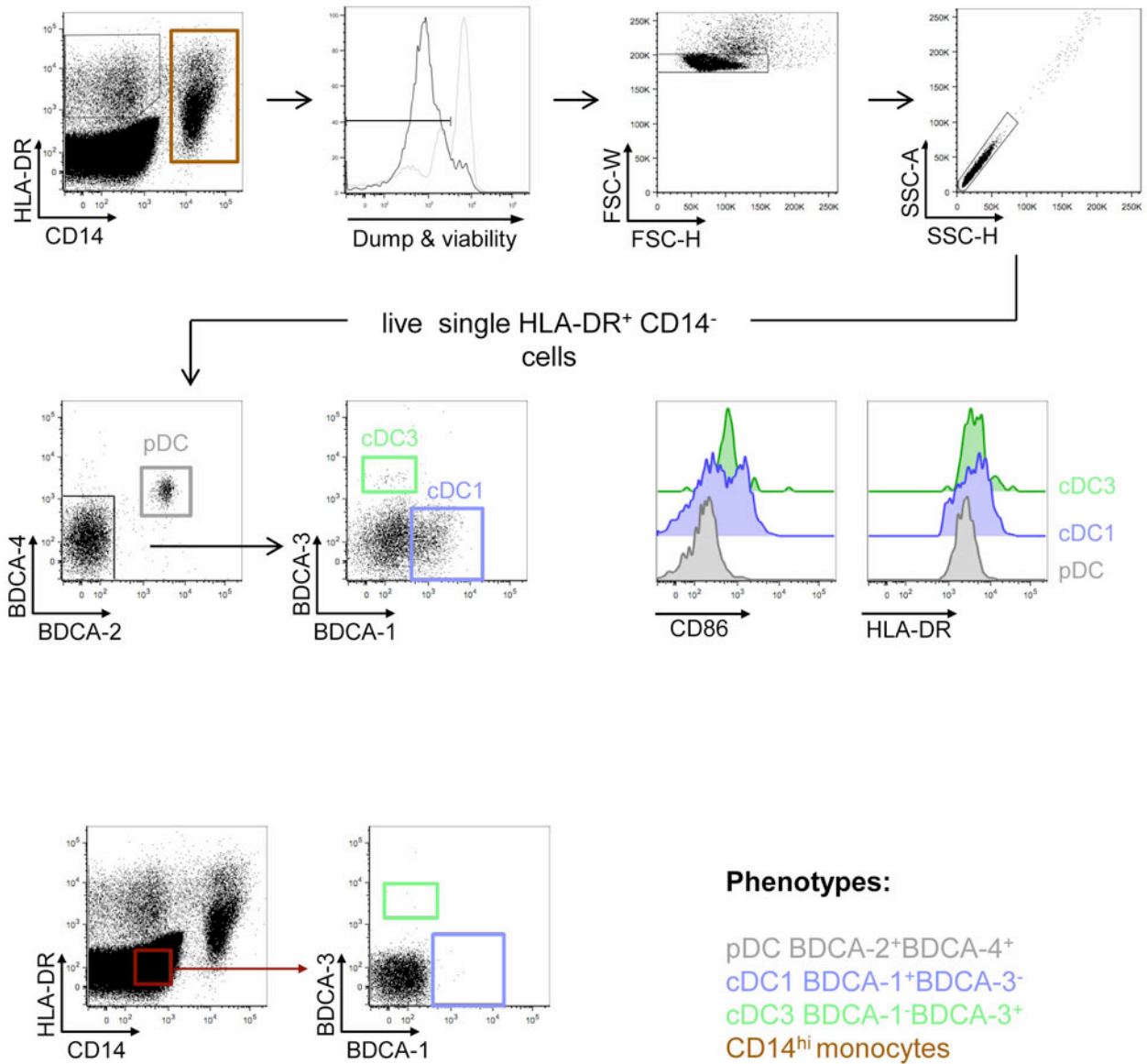
CD32 MFI

CD16 MFI

Supplementary Figure 7

Gating strategy for the PMN cell flow cytometry panel

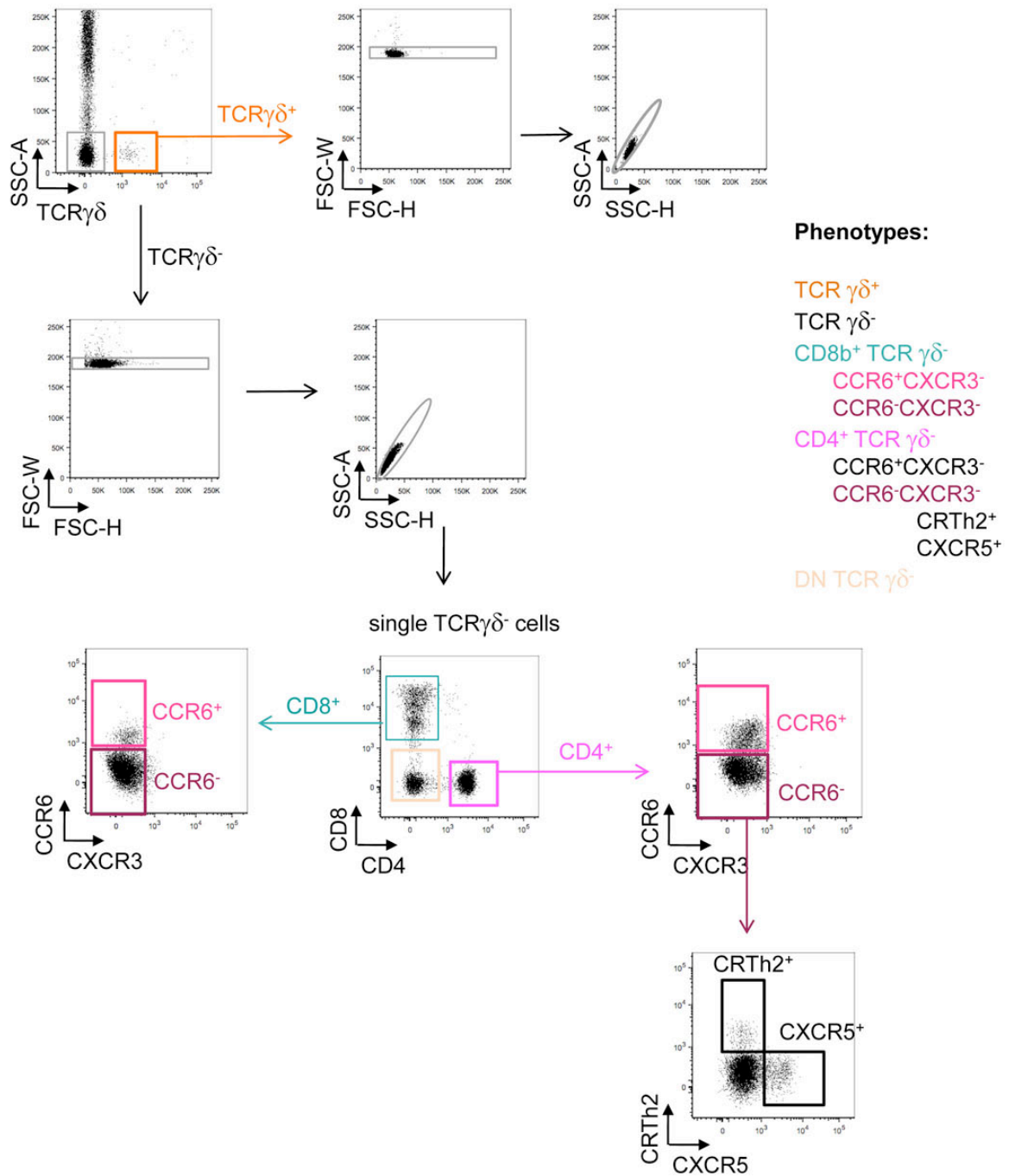
DC panel



Supplementary Figure 8

Gating strategy for the DC flow cytometry panel

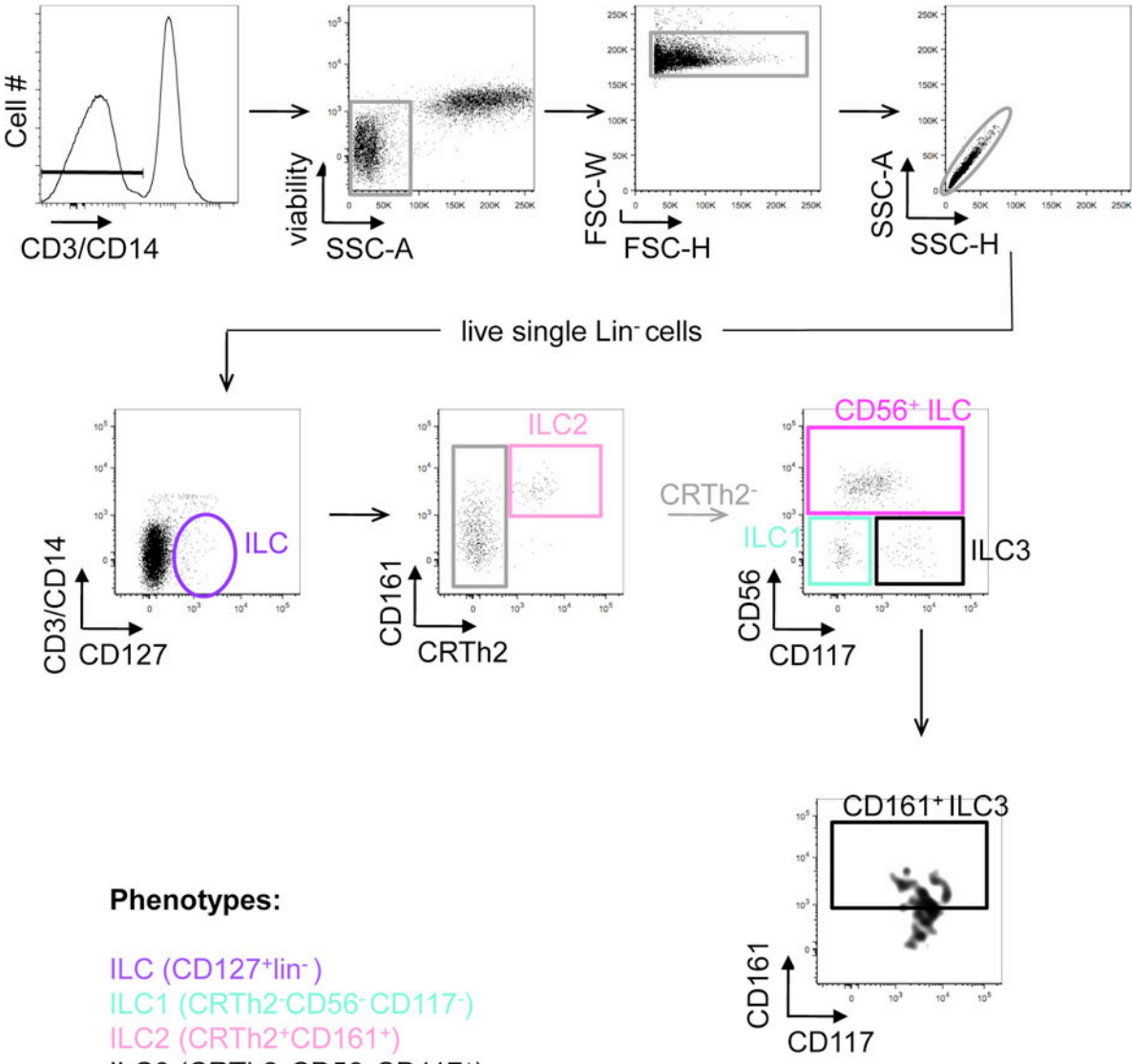
Th panel



Supplementary Figure 9

Gating strategy for the T_H cell flow cytometry panel

ILC panel



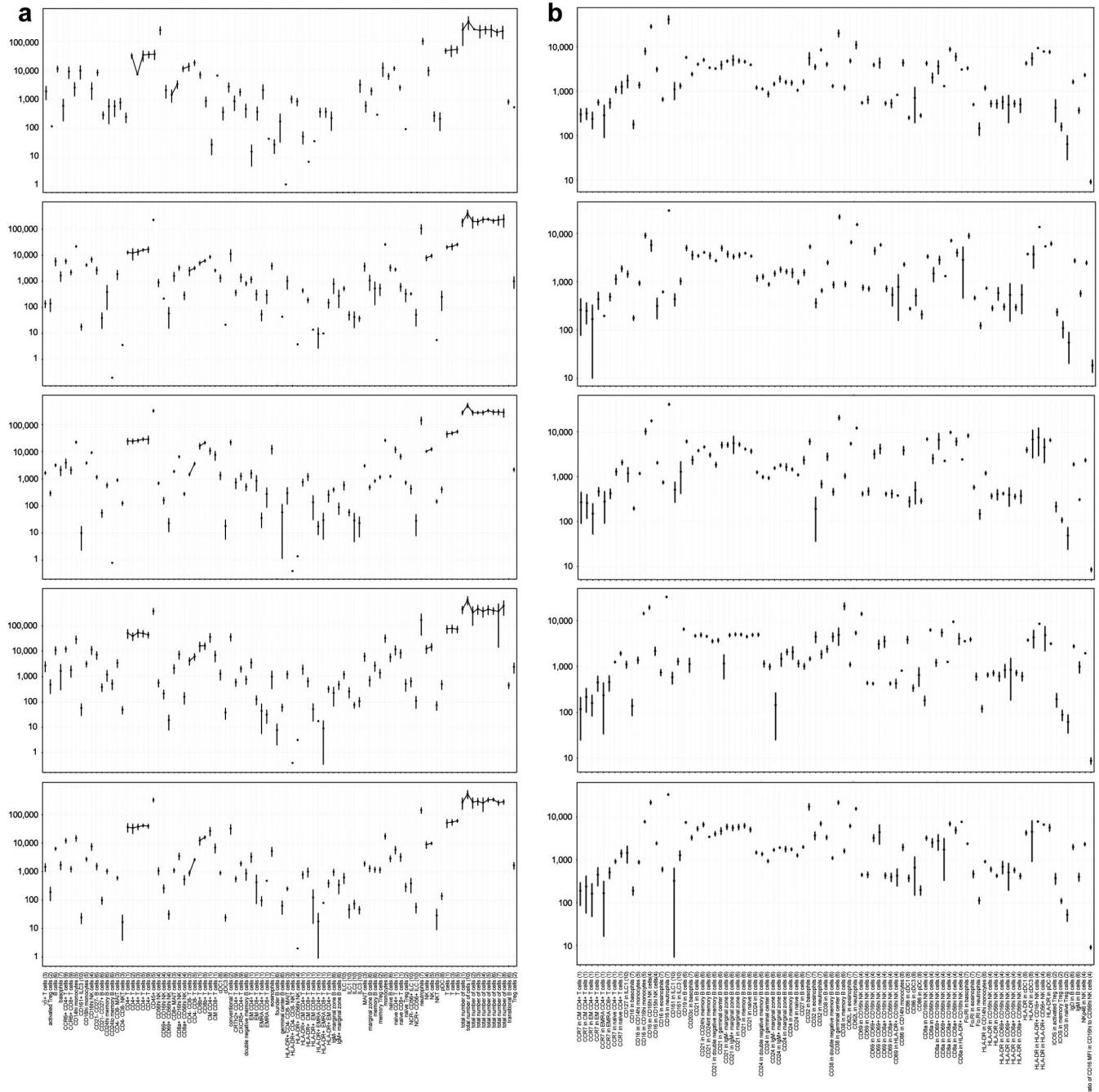
Phenotypes:

- ILC (CD127⁺lin⁻)
- ILC1 (CRTh2⁻CD56⁻CD117⁻)
- ILC2 (CRTh2⁺CD161⁺)
- ILC3 (CRTh2⁻CD56⁻CD117⁺)
- CD56⁺ ILC (CRTh2⁻CD56⁺)

In ILC3:
CD161 MFI

Supplementary Figure 10

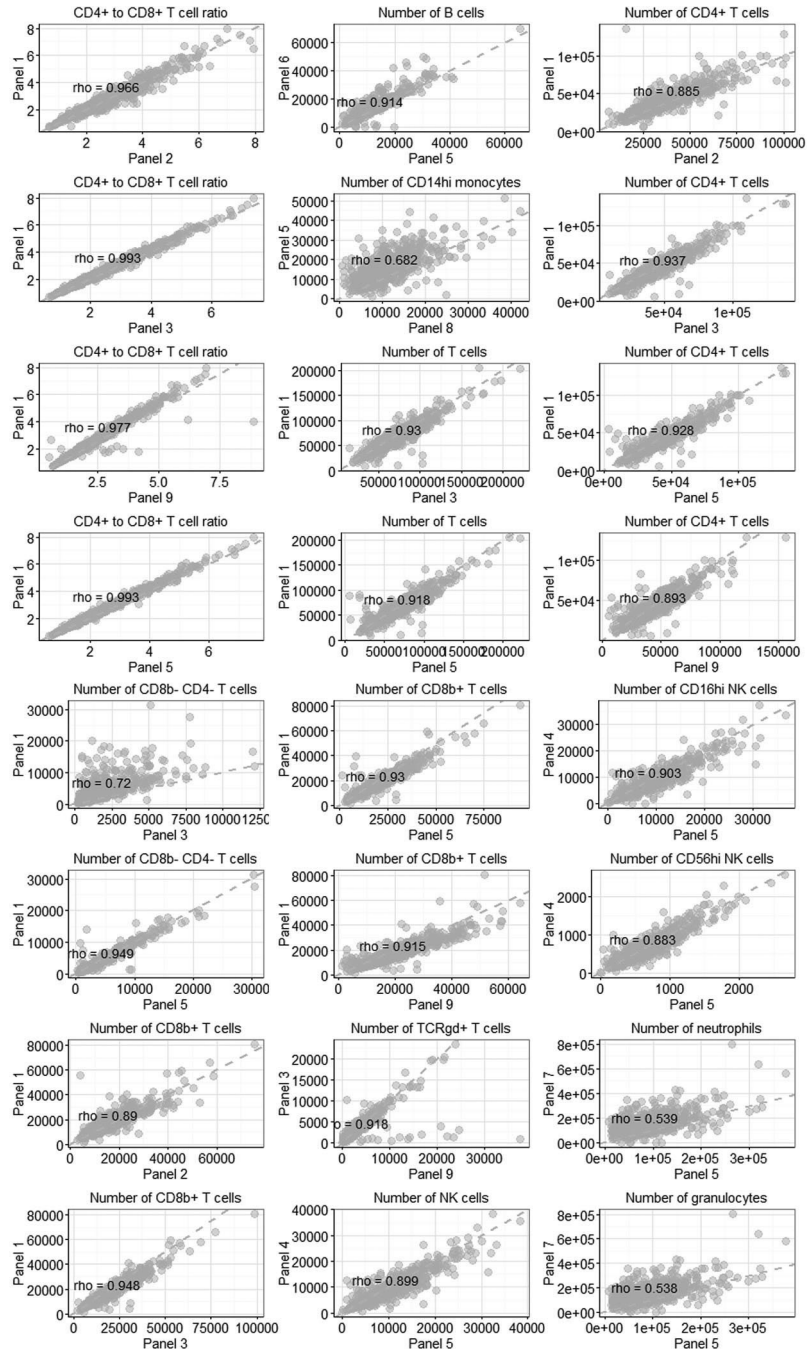
Gating strategy for the ILC flow cytometry panel



Supplementary Figure 12

Repeatability of semi-automated flow cytometry measurements

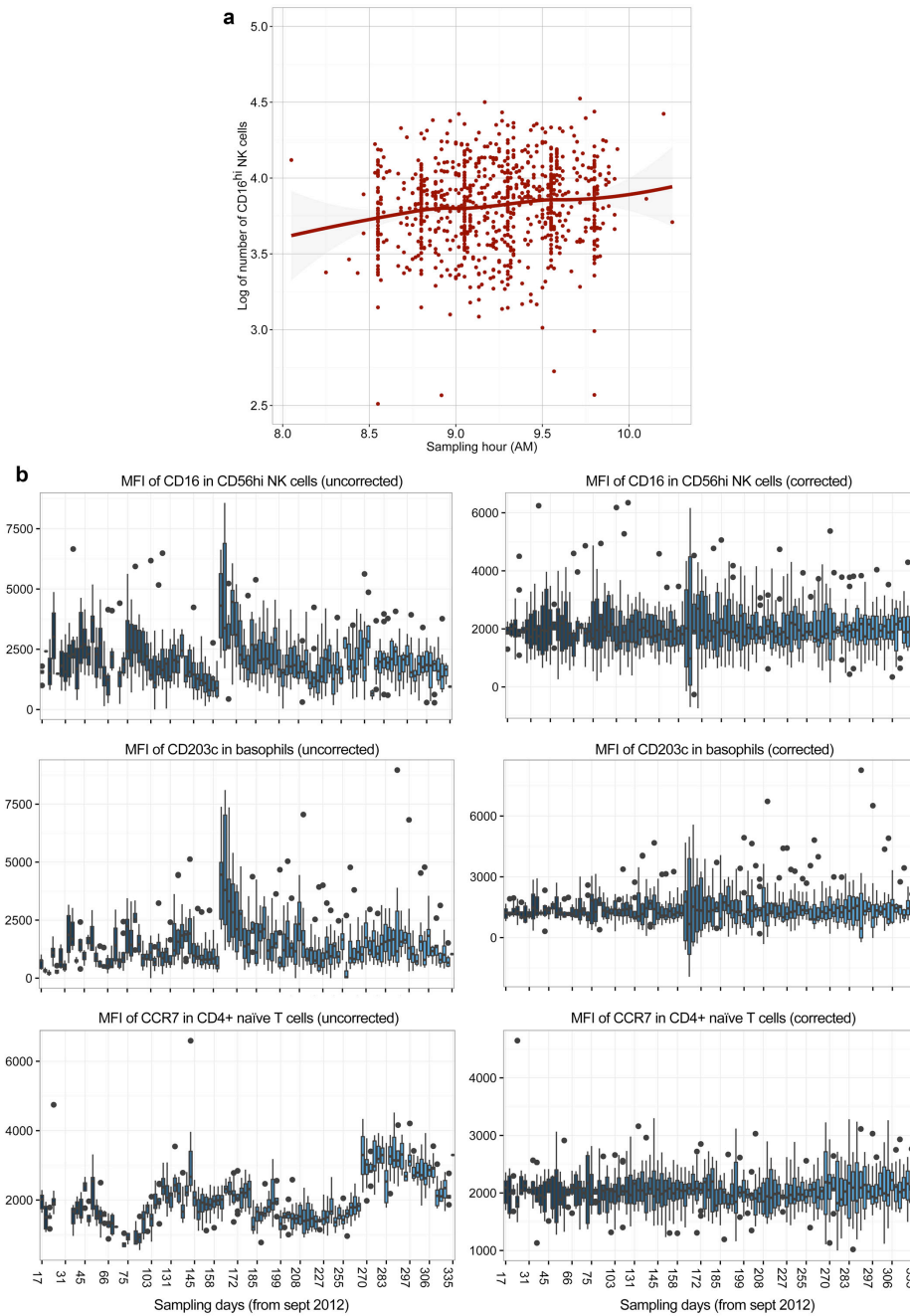
Repeatability of (a) absolute cell counts and (b) MFI estimated based on measurements performed at five different time points over five months on the same five individuals. Points represent the average of measurements across replicates of the same individual, and bars 3 times their standard deviation.



Supplementary Figure 13

Reproducibility of semi-automated flow cytometry measurements

Comparison of cell counts measured in different flow cytometry panels across the 1,000 Milieu Intérieur donors. Spearman's ρ correlation coefficients are shown.



Supplementary Figure 14

Batch effects on measured immunophenotypes

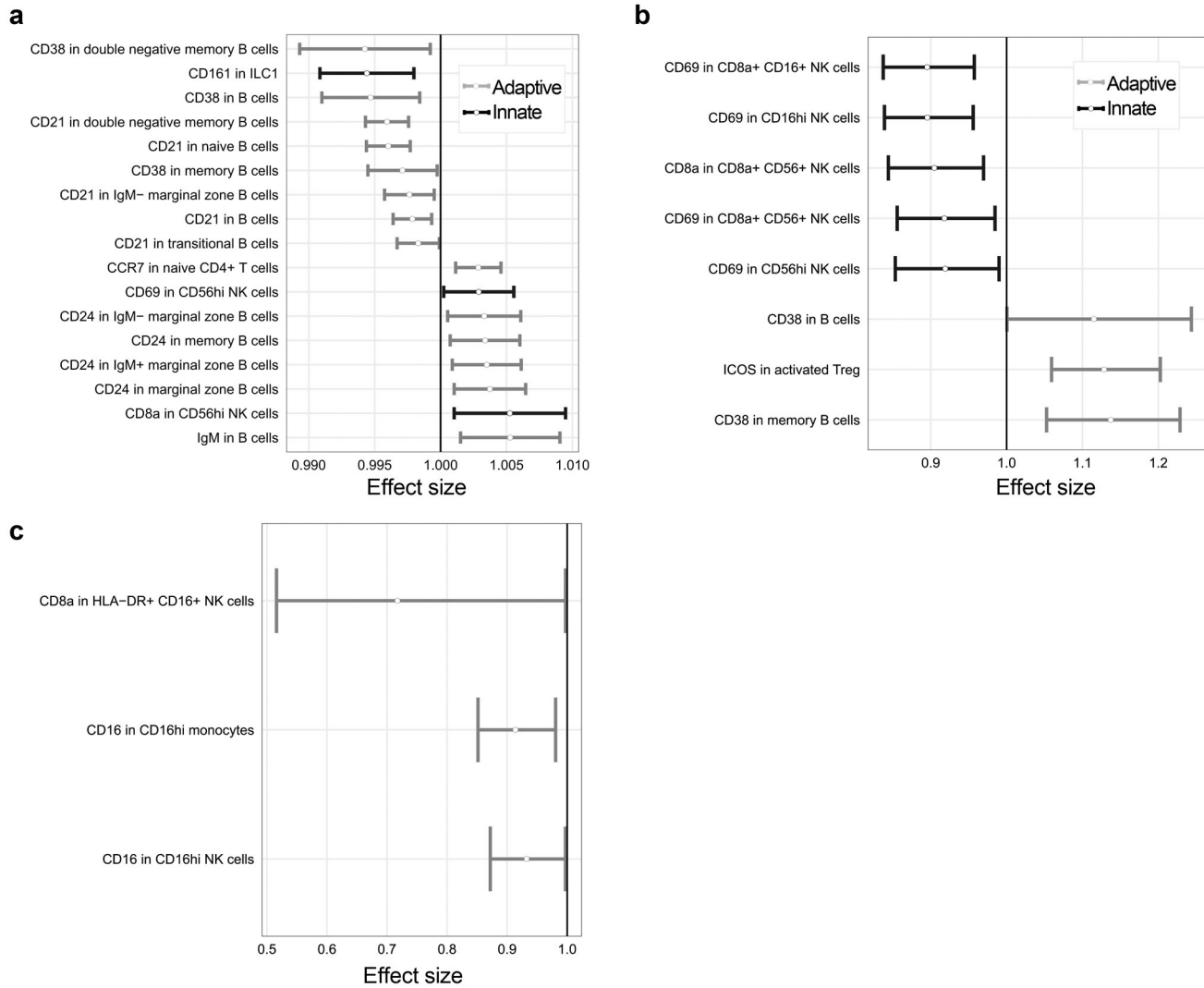
(a) Effect of the sampling hour on the absolute number of CD16^{hi} NK cells. Whole blood samples were collected from the 1,000 Milieu Intérieur healthy subjects every working day from 8 to 11AM. The sampling hour has a significant effect on different immune cell counts, such as the absolute number of CD16^{hi} NK cells, which were adjusted for this batch effect. **(b)** Effect of the sampling day on immunophenotypes measured in the Milieu Intérieur cohort. Whole blood samples were collected from the 1,000 Milieu Intérieur healthy subjects every working day from September 2012 to August 2013. Variation in the mean fluorescence intensity (MFI) of several protein markers was observed along the sampling period. All MFIs were corrected for this batch effect using the ComBat non-parametric Bayesian framework. Three examples of uncorrected (left column) and corrected (right columns) values are shown.



Supplementary Figure 16

Correlations among circulating levels of immune cell populations in the Milieu Intérieur cohort

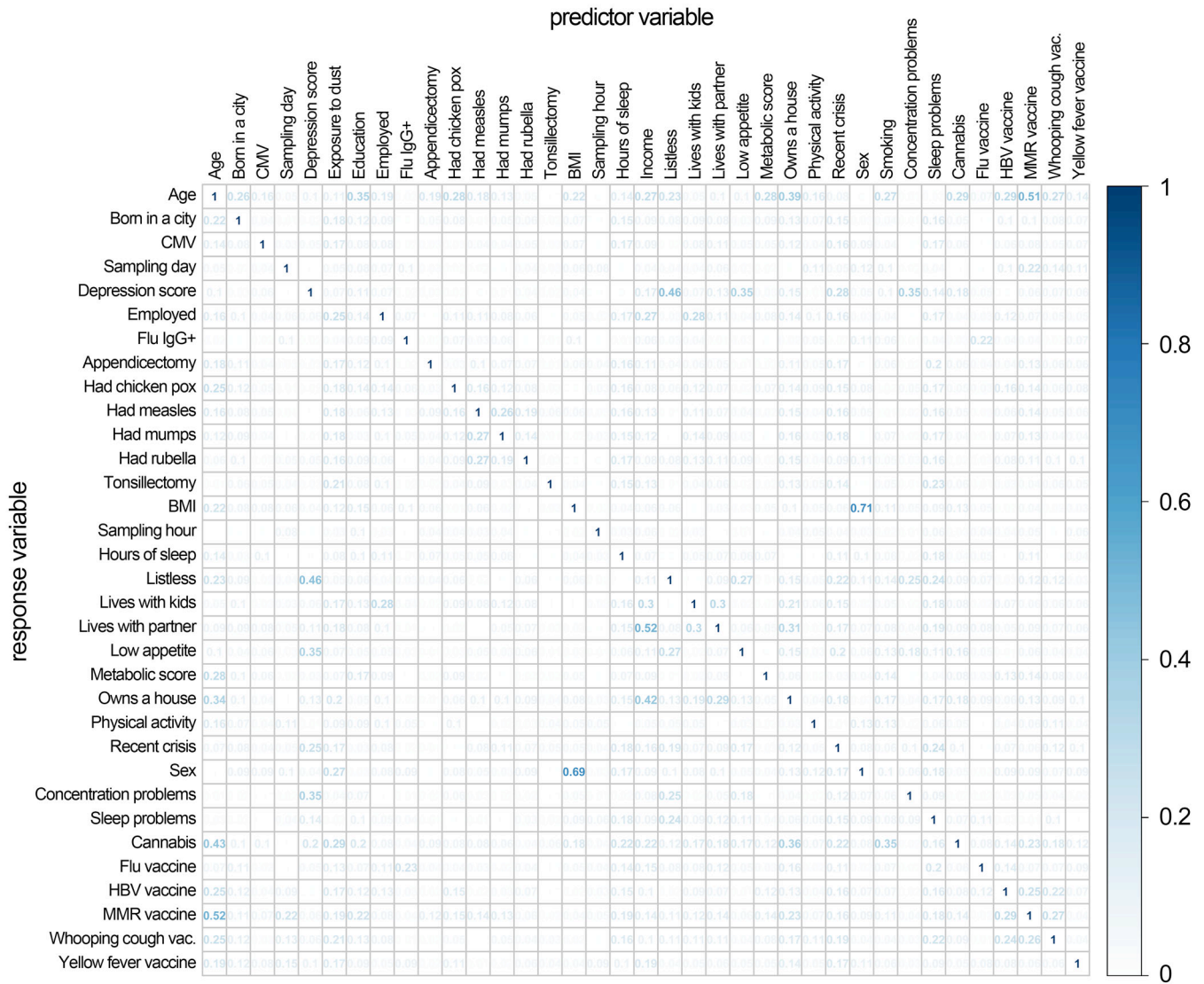
Sample correlations were estimated between the residuals of the log-transformed immunophenotypes from a regression model that included non-genetic covariates selected with the stability selection algorithm (described below) on the 39 non-genetic covariates, together with the batch variables. Correlations between -0.3 and 0.3 were set to 0, to improve readability.

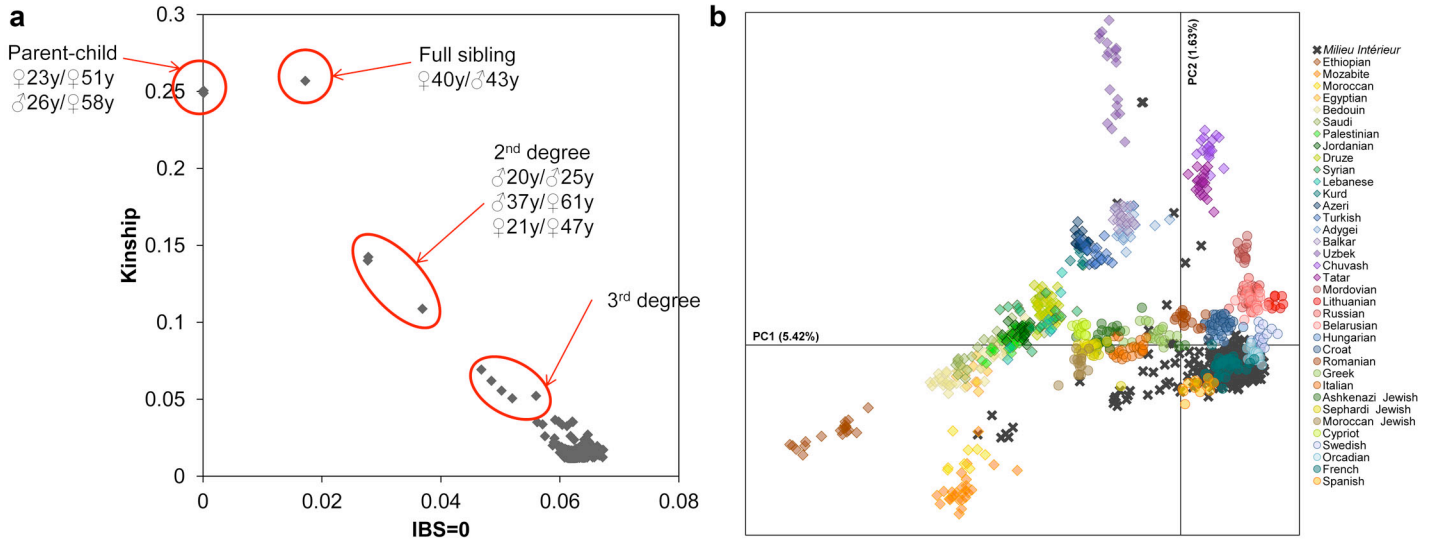


Supplementary Figure 17

Age, sex and CMV infection impact protein levels of immune cell markers in 1,000 healthy individuals

Significant multiplicative effects of (a) increasing age, (b) female sex and (c) CMV seropositivity on the mean fluorescence intensity (MFI) of protein markers of immune cells of 1,000 healthy individuals, controlling for the two other factors, batch effects and genome-wide significant SNPs. The multiplicative effect sizes were estimated in a linear mixed model with a log-transformed response variable, controlling for batch effects and genome-wide significant SNPs, and then transformed to the original data scale. The 99% confidence intervals (99% CIs) were false coverage-adjusted, considering that only 99% CIs of effect sizes with a significant test (adjusted $P < 0.01$) are shown. Adaptive and innate immune cells are represented in grey and black, respectively. These analyses were performed with the *mmi* R package (**Online Methods**).

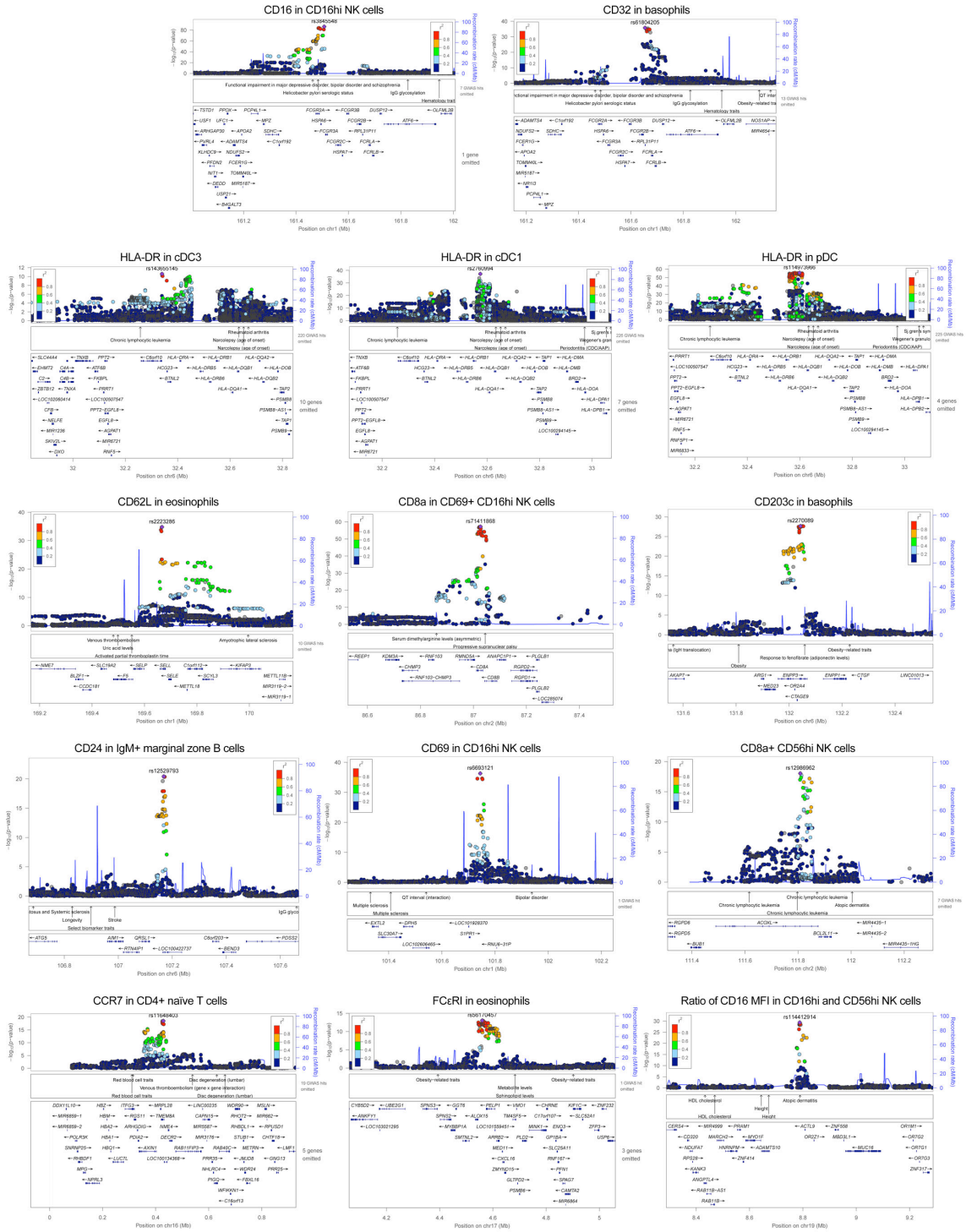




Supplementary Figure 20

Genetic relatedness and structure in the Milieu Intérieur cohort

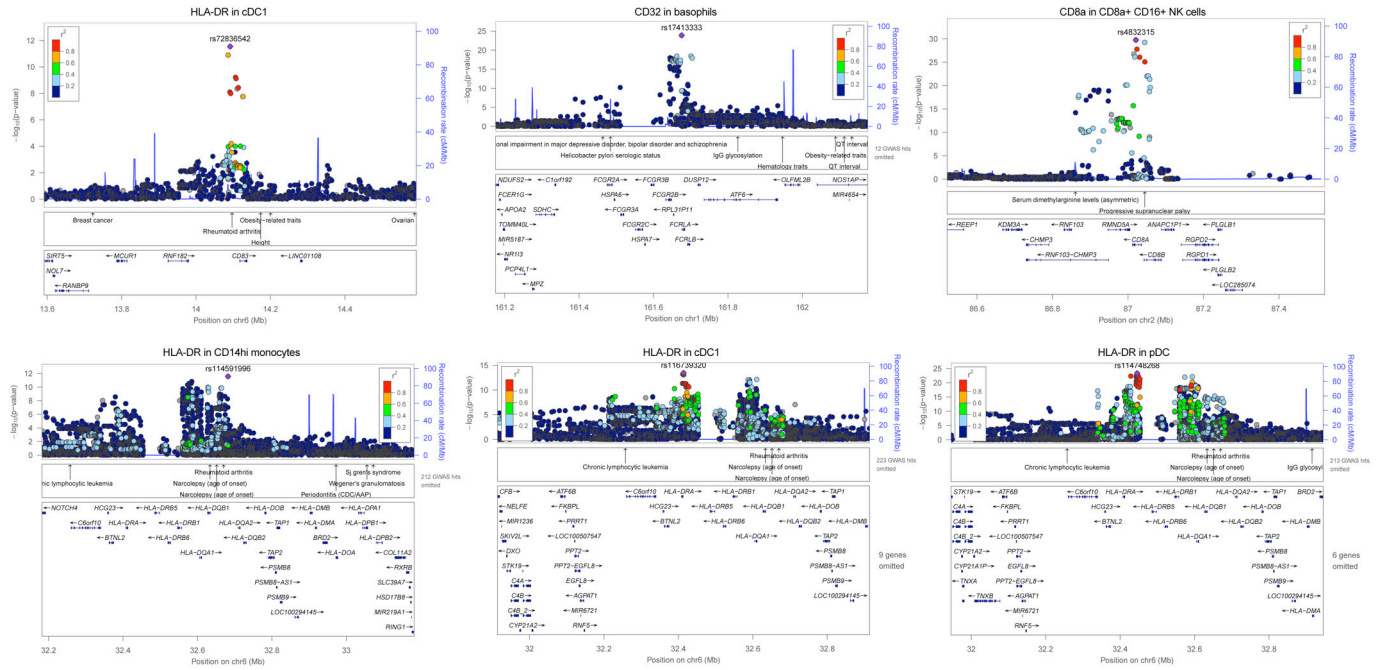
(a) Genetic relatedness in the *Milieu Intérieur* cohort. Pairs of related subjects were detected using an estimate of the kinship coefficient and the proportion of SNPs that are not identical-by-state between all possible pairs of subjects, using KING. (b) Genetic structure of the *Milieu Intérieur* cohort. Genetic structure was estimated with the Principal Component Analysis (PCA) implemented in EIGENSTRAT. For comparison purposes, the analysis was performed on 261,827 independent SNPs and 1,723 individuals, which include the 1,000 *Milieu Intérieur* subjects together with 723 individuals from a selection of 36 populations of North Africa, the Near East, western and northern Europe (**Online Methods**).



Supplementary Figure 21

Local association signals for the 15 genome-wide significant hits associated with immunophenotypes measured in the Milieu Intérieur cohort

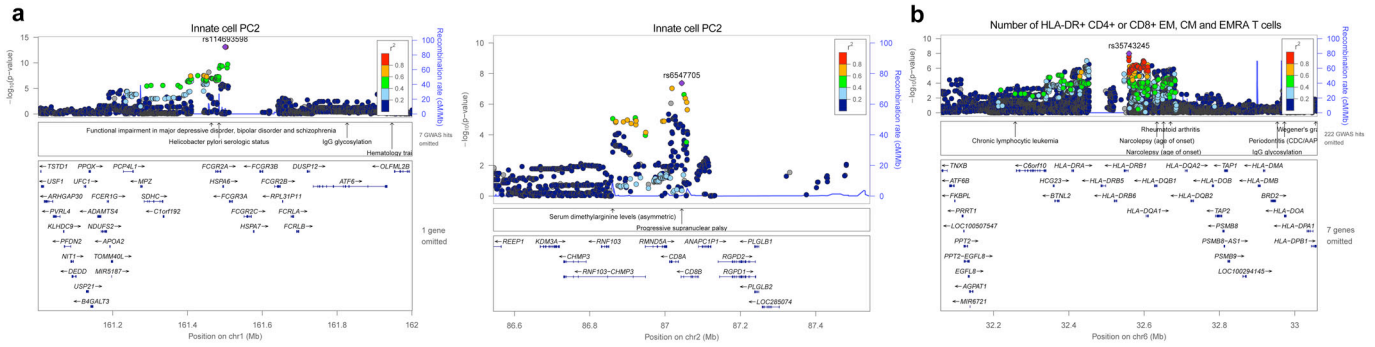
Each point is a SNP, whose color represents its level of linkage disequilibrium (r^2) with the best hit (in purple). Blue lines indicate local recombination rates.



Supplementary Figure 22

Local association signals for the six genome-wide significant hits identified by conditional GWAS of the 15 immunophenotypes showing strong genetic association in the Milieu Intérieur cohort

Each point is a SNP, whose color represents its level of linkage disequilibrium (r^2) with the best hit (in purple). Blue lines indicate local recombination rates. These association signals were identified when conditioning on genotypes of main GWAS signals (**Online Methods**).



Supplementary Figure 23

Local association signals detected by multi-trait GWAS of immunophenotypes measured in the Milieu Intérieur cohort

(a) Local association signals at loci influencing principal components of a PCA of all innate cell immunophenotypes. No suggestive signal ($P < 5 \times 10^{-8}$) was observed for PCs of a PCA of adaptive cell immunophenotypes. (b) Local association signal with the absolute numbers of HLA-DR⁺ T_{CM}, T_{EM} and T_{EMRA} cells, either CD4⁺ or CD8⁺. The six corresponding immunophenotypes were analyzed altogether using a multivariate GWAS (Online Methods).